Article

Calibration of Nonstationary Gas Sensors Based on Two-Dimensional Materials

Filiberto Ricciardella,* Kangho Lee, Tobias Stelz, Oliver Hartwig, Maximilian Prechtl, Mark McCrystall, Niall McEvoy, and Georg S. Duesberg*

Cite This: *ACS Omega* 2020, 5, 5959−5963

Read Online

ACCESS | 📊 Metrics & More | 📄 Article Recommendations | 🆘 Supporting Information

ABSTRACT: Two-dimensional materials (2DMs) have high potential in gas sensing, due to their large surface-to-volume ratio. However, most sensors based on 2DMs suffer from the lack of a steady state during gas exposure, hampering sensor calibration. Here, we demonstrate that analysis of the time differential of the signal output enables the calibration of chemiresistors based on platinum or tungsten diselenide ($PtSe_2$, WSe_2) and molybdenum disulfide (MoS_2), which present nonstationary behavior. 2DMs are synthesized by thermally assisted conversion of predeposited metals on a silicon/silicon dioxide substrate and therefore are integrable with standard complementary metal−oxide semiconductor (CMOS) technology. We analyze the behavior of the sensors at room temperature toward nitrogen dioxide (NO_2) in a narrow range from 0.1 to 1 ppm. This study overcomes the problem of the absence of steady-state signals in 2DM gas sensors and thus facilitates their usage in this highly important application.
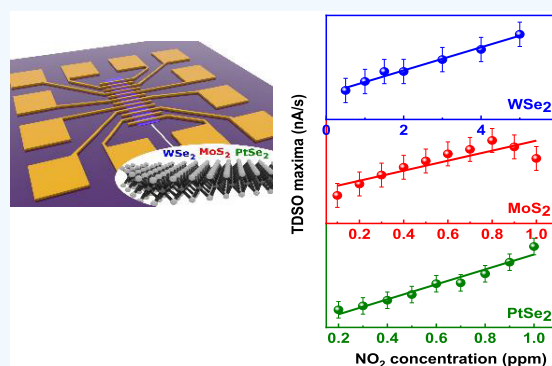
INTRODUCTION

The monitoring of toxic and flammable gases at low concentration is challenging, especially in domestic and industrial environments.[1] Among the waste species produced nowadays, nitrogen dioxide (NO_2) represents one of the most common exhaust gases as it is usually obtained from numerous industrial applications. This oxidizing gas can have a severe effect on human health, particularly in terms of permanent damage to the respiratory system, even at concentration levels as low as 1 ppm (parts per million).[2,3] As such, gas sensors capable of detecting extremely low concentrations are highly sought after.[4] Over the previous few decades, metal oxides (MO_x) have shown their potential as sensing materials due to their high sensitivity to pollutant gases, small size of devices, and low cost.[1,5] However, it is known that MO_x-based sensors only perform well when working at temperatures typically higher than 400 °C, with consequent huge consumption of energy.[5−8]

Sensors based on low-dimensional materials, including carbon nanotubes, graphene, and black phosphorus, have been widely investigated as promising alternatives to MO_x.[2,9−15] Semiconducting two-dimensional (2D) transition metal dichalcogenides (TMDCs) have been widely investigated as promising gas-sensing materials due to their high surface-to-volume ratio, favorable surface energy levels for gas adsorption, high mobilities, and high current on/off ratios.[16−19] A number of TMDCs have shown low detection limits for NO_2 operating at room temperature (RT).[19−23]

Recently, platinum diselenide ($PtSe_2$) has gained huge interest for selective NO_2 sensing with a low limit of detection (LOD) in the range of few ppb and an extremely fast response time (few seconds) when exposed to 0.1 ppm.[24,25]

However, most gas sensors based both on TMDCs and other low-dimensional materials suffer significantly from drawbacks such as the lack of a steady state during the gas exposure and slow recovery kinetics. These two hindrances can hamper the use of sensors since two characteristic parameters, the response time and the signal variation, cannot be properly determined.[26,27] In previous reports,[28−30] we have demonstrated that the limitations can be overcome simply by analyzing the time differential of the signal output (TDSO) instead of the output itself. In those papers, the sensing material consisted of multilayered graphene (MLG), synthesized through different routes.

Here, we demonstrate the reliability of the TDSO approach applying it to chemiresistors (CRs) based on three different TMDCs: platinum diselenide ($PtSe_2$), tungsten diselenide (WSe_2), and molybdenum disulfide (MoS_2). The sensors show continuously rising current during a gas exposure longer than 2

min, similar to those based on MLG.[28−31] By means of TDSO, we are able to properly calibrate and compare the sensors, highlighting the promising potentialities of these materials in the field of gas sensors working at room temperature (RT).

RESULTS AND DISCUSSION

Raman and X-ray photoelectron spectroscopy (XPS) results reported in our previous publications show the stochiometric transformation of Pt, Mo, and W into $PtSe_2$, MoS_2, and WSe_2, respectively, by thermally assisted conversion (TAC).[20−22,25,32−34] Here, we present the application of TDSO to the devices based on TMDCs reported in those papers, in which a detailed characterization of TMDCs is presented.

Figure 1 shows the optical images and the current−voltage ($I−V$) characteristics of the devices based on the aforemen-
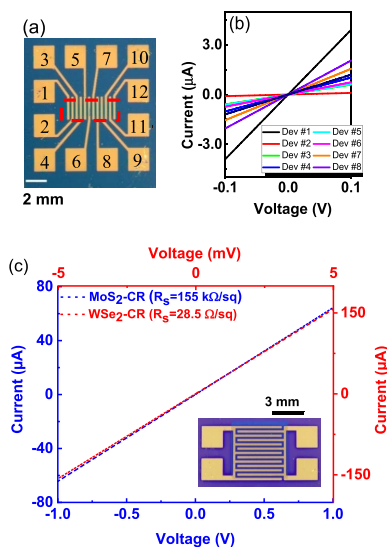

Figure 1. (a) Optical image of the chip containing the eight devices based on $PtSe_2$ with labeled pads. The dashed red rectangle surrounds the $PtSe_2$ film. (b) $I−V$ characteristics of the $PtSe_2$-based resistors reported in Table S1. (c) $I−V$ characteristics of the resistors based on MoS_2 (blue line) and WSe_2 (red line). Inset: sketch of the MoS_2 (WSe_2) sensor.

tioned TMDCs. The linearity of the $I−V$ characteristics (Figure 1b,c) recorded for the investigated devices suggests that the possibility that Schottky barriers at the contacts to the $PtSe_2$, MoS_2, and WSe_2 films can be excluded. For the $PtSe_2$-based devices, the values of sheet resistance (R_S) are in the range of a few hundred kΩ/sq (Table 1). The variance of the resistance values can likely be attributed to thickness variation and roughness of the sputtered Pt film at the nanoscale level.

Figure 2a illustrates the real-time current behavior (black line) of $PtSe_2$-CR #1 upon sequential exposures of NO_2 (red rectangles). The signals recorded for the other tested $PtSe_2$-based devices are shown in the Supporting Information (Figure S1).

In each exposure window, the current shows an increasing signal, never reaching the stationary state, especially for NO_2 concentrations higher than 0.5 ppm. Similar results are reported elsewhere.[28−31] The lack of a steady state is more evident in Figure 2b, where the signals recorded upon exposure to different concentrations are grouped. It can be seen that the variation of the current toward 100 ppb of NO_2 (black curve)

Table 1. Differential Sensitivity (DS) of $PtSe_2$-Based Sensors

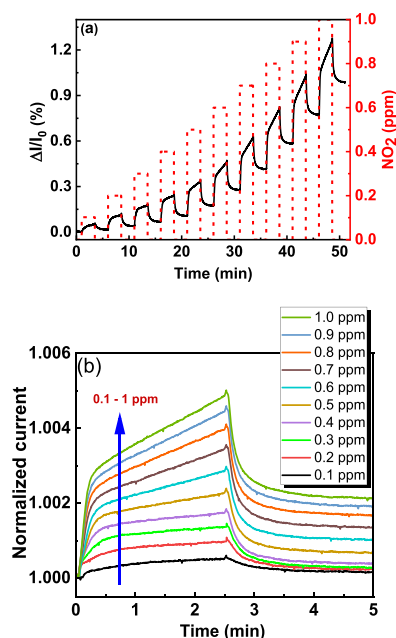| device	differential sensitivity [nA/(s·ppm)]
#1	0.91 ± 0.07
#2	0.93 ± 0.07
#3	0.82 ± 0.11
#4	0.83 ± 0.06
#5	0.93 ± 0.06
#6	0.99 ± 0.08
#7	0.88 ± 0.04
#8	0.80 ± 0.04

Figure 2. (a) Real-time current behavior (black curve) of $PtSe_2$-CR #1 during exposure to increasing concentrations of NO_2 (red dashed rectangles). Dry N_2 is used as a buffer gas. (b) Signals recorded upon exposure to different concentrations of NO_2. The current is normalized at the value reached when each gas exposure starts.

is almost negligible compared to the others at higher concentrations.

Figure 2b also shows that the higher the concentration of the injected gas, the smaller the return of the current to the initial state. Noteworthily, based on the definition of the term "recovery" as the time required to reduce the stationary signal value by 90%,[26] we need to carefully adopt this term to describe the restoration of the signal after the gas pulse. At concentrations lower than 0.5 ppm, the current value is almost restored to the initial value in 150 s. When the sensor is exposed to the highest concentration (1 ppm), for instance, the current is lowered by less than 30% from the value reached when the gas is removed. These outcomes straightforwardly point out two features: first, the continuous integrating capability of the sensors and second, the difficulty in removing the adsorbed molecules in a timescale feasible for applications in environmental conditions.[28] These two limitations, which commonly affect the sensors based on 2D materials, are mathematically overcome by the TDSO approach.[28] In Figure 3a, the method is applied to the signal recorded on device #1. The TDSO (red curve) is overlapped upon the transients of the sensor (black line), where I_0 and I represent the values of
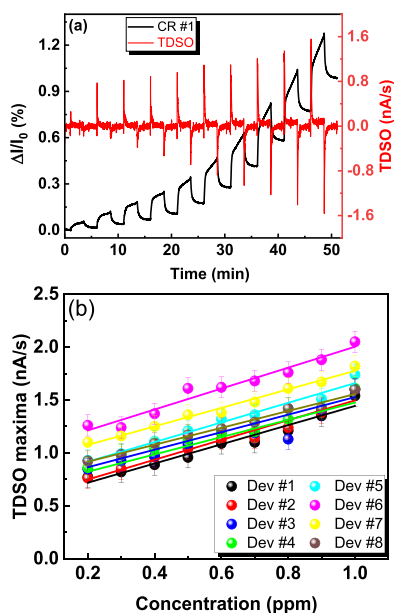
Figure 3. (a) Real-time percentage current variation (black curve) of CR #1 during the exposure to increasing concentrations of NO_2 and corresponding TDSO (red curve). Analogous results are obtained for the other seven devices (see the Supporting Information). (b) Maxima of the differential curves determined for the eight devices (see the Supporting Information) and plotted as a function of the NO_2 concentration.

Figure 4. Calibration curves of (a) MoS_2- and (b) WSe_2-based CR. The insets show the transients upon sequential NO_2 exposures and TDSO, respectively, in black and red.

the current when the gas is injected and stopped, respectively, during each exposure. The TDSO peaks are well distinguishable for each gas pulse except at 0.1 ppm (Figure 3a).

At that concentration, the peak is not well visible because of the small variation of the signal (Figure 2b). As the rise time of the sensor is in the range of tens of seconds, the TDSO peaks are located quite close to the position of the gas inlet (t_0), as mathematically modeled in ref 28 (Figure S2).

The maxima of TDSO plotted as a function of the NO_2 concentration in the range 0.2−1.0 ppm (Figure 3b) display comparable behavior for the complete set of sensors, especially in terms of linearity of the fitting curves. To properly compare the performance of the sensors, the most powerful tool is differential sensitivity (DS), defined as the slope of the calibration curve.[28] Further studies are ongoing to address the definition of the limit of detection through the TDSO approach. For the eight devices investigated in this paper, the values of the DS are comparable within a maximum variation of about 20% (Table 1).

To further prove the reliability of the TDSO approach, we tested CRs based on MoS_2 and WSe_2. Figure 4 reports the calibration curves obtained by applying TDSO on both sensors. For MoS_2-CR (Figure 4a), the peaks were determined from the same test protocol (inset of Figure 4a) used for $PtSe_2$-CRs. WSe_2-CR, instead, was revealed to be scarcely sensitive to NO_2 concentrations lower than 0.4 ppm, showing no intense TDSO peaks (inset of Figure 4b). As such, we slightly modified the protocol, exposing the WSe_2-CR up to 5 ppm of NO_2.

Because of the decreasing current shown by both sensors, we reported the absolute values of the TDSO peaks as a function of the NO_2 concentration. The n- or p-type behavior of MoS_2 is already shown in other reports,[22,35,36] while we are further investigating the behavior of WSe_2. Nevertheless, in the present
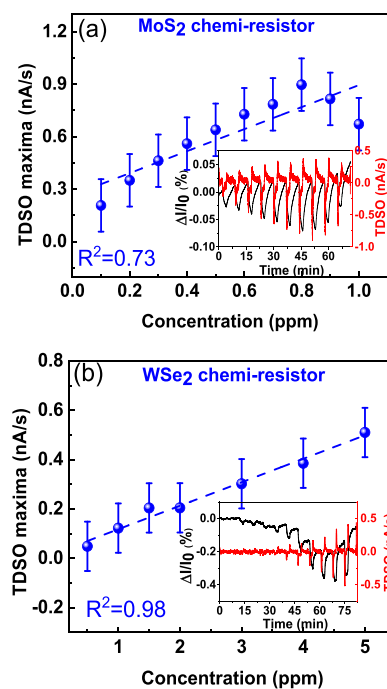
paper, we mostly focus on TDSO to overcome the calibration issue. The linearity of the calibration curve first confirms the reliability of the TDSO approach. The DS of MoS_2-CR (0.6 ± 0.1 nA/(s·ppm)) indicates that TAC-grown MoS_2 is slightly more sensitive than TAC-grown $PtSe_2$ toward NO_2 in the investigated range.

A fairer comparison between the results presented here and those reported in the literature can be based on the minimum detectable concentration of gas. Except for the WSe_2-based CR, the sensors presented here are able to distinguish down to a hundred ppb of NO_2 working at RT. These findings are in close agreement with up to date results.[16,25,37] By further refinement of the materials synthesis route, it is very likely that the detectable gas concentration will be lowered significantly.

■ CONCLUSIONS

We have analyzed the sensing properties of chemiresistors based on $PtSe_2$, MoS_2, and WSe_2 toward NO_2. The devices were able to detect concentrations of NO_2 in N_2 down to few hundred ppb at RT. We addressed the issue of a nonstationary state shown during the gas exposure by applying the TDSO approach. We definitively proved that the maxima of TDSO are uniquely and linearly correlated with the NO_2 concentration in the range 0.1−1 ppm. The TDSO approach allowed us to properly calibrate the sensors based on three different TMDCs, showing the potential of these materials in the field of gas sensors operating at RT.

■ EXPERIMENTAL SECTION

Films of $PtSe_2$, MoS_2, and WSe_2 were synthesized by thermally assisted conversion (TAC) of Pt, Mo, and W, respectively. Thin layers of Pt (0.5 nm), Mo (10 nm), and W (20 nm) were sputtered onto SiO_2 (300 nm)/Si substrates. The samples were then loaded into a quartz tube furnace and heated at 400, 750, and 600 °C, respectively. The vapors of the chalcogens were

produced at ~115 °C (S) and ~220 °C (Se) and diffused into the metal layers to form PtSe$_2$, MoS$_2$, and WSe$_2$, respectively. The TAC process is described in detail in previous reports.[20,21,25]

To fabricate the gas sensors, we used shadow masks to sputter Pt, Mo, and W layers only on selected areas. After the synthesis of patterned PtSe$_2$, MoS$_2$, and WSe$_2$ by the TAC process, metal contacts (Ni/Au for PtSe$_2$ or WSe$_2$, Ti/Au for MoS$_2$) were deposited using hard masks to define the sensing areas.[21,25] For instance, Figure 1 illustrates the PtSe$_2$-based CRs. Each device is about 1 × 0.2 mm^2. The electrical measurements were performed using a Keithley 2636 Source Meter Unit and a Keithley 3706 System Switch/Multimeter. We tested the gas sensors based on TMDC in a custom-made chamber with a volume of about 10 cL and remote-controllable mass-flow controllers (MFCs). The pressure and temperature were kept constant at 150 Torr and room temperature (RT). A constant flow of the gas mixture (100 sccm) was flushed in the chamber. We injected 10 ppm of NO$_2$ into the test chamber, diluting it with dry nitrogen (N$_2$) to achieve concentrations ranging from 0.1 to 1 ppm. Each of the ten gas pulses and subsequent recovery steps lasted 150 s. The sensors were biased at 1 V. The resistance of the devices upon the periodic gas exposure was simultaneously monitored.

■ ASSOCIATED CONTENT

Ⓢ Supporting Information

The Supporting Information is available free of charge at https://pubs.acs.org/doi/10.1021/acsomega.9b04325.

Sheet resistance (R_s) values of PtSe$_2$-based resistors; real-time current behavior and TDSO of PtSe$_2$-based chemiresistors(CR) upon sequential exposures of NO$_2$; zoom on the current signal upon NO$_2$ pulse at 1 ppm; the corresponding TDSO; signals recorded by PtSe$_2$-CR #1 upon exposure to different concentrations (PDF)

■ AUTHOR INFORMATION

Corresponding Authors

Filiberto Ricciardella − *Institute for Physics, EIT 2, Bundeswehr University Munich, 85577 Neubiberg, Germany;* ⓞ orcid.org/0000-0002-9669-5649; Email: filiberto.ricciardella@gmail.com

Georg S. Duesberg − *Institute for Physics, EIT 2, Bundeswehr University Munich, 85577 Neubiberg, Germany;* Email: duesberg@unibw.de

Authors

Kangho Lee − *Institute for Physics, EIT 2, Bundeswehr University Munich, 85577 Neubiberg, Germany*

Tobias Stelz − *Institute for Physics, EIT 2, Bundeswehr University Munich, 85577 Neubiberg, Germany*

Oliver Hartwig − *Institute for Physics, EIT 2, Bundeswehr University Munich, 85577 Neubiberg, Germany*

Maximilian Prechtl − *Institute for Physics, EIT 2, Bundeswehr University Munich, 85577 Neubiberg, Germany*

Mark McCrystall − *School of Physics, Trinity College Dublin, Dublin 2, Ireland*

Niall McEvoy − *Advanced Materials and Bioengineering Research Centre (AMBER) and School of Chemistry, Trinity College Dublin, Dublin 2, Ireland;* ⓞ orcid.org/0000-0001-5950-8755

Complete contact information is available at:

Author Contributions

F.R. conceived the idea, analyzed the data, and wrote the manuscript. K.L. performed the sensing measurements. T.S. assisted in plotting the data and formatted the manuscript. O.H. and M.P. performed the material characterization. M.M. and N.M. synthesized the material, and G.S.D. supervised the manuscript. All authors provided their own contribution in writing the manuscript.

Notes

The authors declare no competing financial interest.

■ REFERENCES

(1) Anukunprasert, T.; Saiwan, C.; Traversa, E. The Development of Gas Sensor for Carbon Monoxide Monitoring Using Nanostructure of Nb-TiO2. *Sci. Technol. Adv. Mater.* **2005**, *6*, 359−363.

(2) Wu, E.; Xie, Y.; Yuan, B.; Zhang, H.; Hu, X.; Liu, J.; Zhang, D. Ultrasensitive and Fully Reversible NO$_2$ Gas Sensing Based on P-Type MoTe2 under Ultraviolet Illumination. *ACS Sens.* **2018**, *3*, 1719−1726.

(3) Ricciardella, F. From graphene to graphene-based gas sensors operating in environmental conditions. Ph.D. Thesis, Università degli Studi di Napoli Federico II, 2015.

(4) Baron, R.; Saffell, J. Amperometric Gas Sensors as a Low Cost Emerging Technology Platform for Air Quality Monitoring Applications: A Review. *ACS Sens.* **2017**, *2*, 1553−1566.

(5) Liu, Y.; Parisi, J.; Sun, X.; Lei, Y. Solid-State Gas Sensors for High Temperature Applications − a Review. *J. Mater. Chem. A* **2014**, *2*, 9919−9943.

(6) Kim, H.; Lee, J. Sensors and Actuators B : Chemical Highly Sensitive and Selective Gas Sensors Using p-Type Oxide Semi-conductors : Overview. *Sens. Actuators, B* **2014**, *192*, 607−627.

(7) Dey, A. Semiconductor Metal Oxide Gas Sensors: A Review. *Mater. Sci. Eng. B* **2018**, *229*, 206−217.

(8) Arshak, K.; Moore, E.; Lyons, G. M.; Harris, J.; Clifford, S. A Review of Gas Sensors Employed in Electronic Nose Applications. *Sens. Rev.* **2004**, *24*, 181−198.

(9) Nag, A.; Mitra, A.; Chandra, S. Sensors and Actuators A : Physical Graphene and Its Sensor-Based Applications : A Review. *Sens. Actuators, A* **2018**, *270*, 177−194.

(10) Llobet, E. Gas Sensors Using Carbon Nanomaterials: A Review. *Sens. Actuators, B* **2013**, *179*, 32−45.

(11) Iqbal, N.; Afzal, A.; Cioffi, N.; Sabbatini, L.; Torsi, L. NOx Sensing One- and Two-Dimensional Carbon Nanostructures and Nanohybrids: Progress and Perspectives. *Sens. Actuators, B* **2013**, *181*, 9−21.

(12) Abbas, A. N.; Köpf, M.; Ma, Y.; Nilges, T.; Cong, S.; Chen, L.; Zhou, C.; Aroonyadet, N.; Liu, B. Black Phosphorus Gas Sensors. *ACS Nano* **2015**, *9*, 5618−5624.

(13) Donarelli, M.; Prezioso, S.; Perrozzi, F.; Bisti, F.; Nardone, M.; Giancaterini, L.; Cantalini, C.; Ottaviano, L. Response to NO$_2$ and Other Gases of Resistive Chemically Exfoliated MoS$_2$-Based Gas Sensors. *Sens. Actuators, B* **2015**, 602−613.

(14) Kannan, P. K.; Late, D. J.; Morgan, H.; Rout, C. S. Recent Developments in 2D Layered Inorganic Nanomaterials for Sensing. *Nanoscale* **2015**, *7*, 13293−13312.

(15) Jaiswal, J.; Sanger, A.; Tiwari, P.; Chandra, R. MoS$_2$ Hybrid Heterostructure Thin Film Decorated with CdTe Quantum Dots for Room Temperature NO2 Gas Sensor. *Sens. Actuators, B* **2020**, *305*, No. 127437.

(16) Mao, S.; Chang, J.; Pu, H.; Lu, G.; He, Q.; Zhang, H.; Chen, J. Two-Dimensional Nanomaterial-Based Field-Effect Transistors for Chemical and Biological Sensing. *Chem. Soc. Rev.* **2017**, *46*, 6872−6904.

(17) Yang, W.; Gan, L.; Li, H.; Zhai, T. Two-dimensional layered nanomaterials for gas-sensing applications. *Inorg. Chem. Front.* **2016**, *3*, 433−451.

(18) Zhao, Y.; Qiao, J.; Yu, Z.; Yu, P.; Xu, K.; Lau, S. P.; Zhou, W.; Liu, Z.; Wang, X.; Ji, W.; et al. High-Electron-Mobility and Air-Stable 2D Layered PtSe$_2$ FETs. *Adv. Mater.* **2017**, *29*, No. 1604230.

(19) Anichini, C.; Czepa, W.; Pakulski, D.; Aliprandi, A.; Ciesielski, A.; Samorì, P. Chemical Sensing with 2D Materials. *Chem. Soc. Rev.* **2018**, *47*, 4860−4908.

(20) Gatensby, R.; Hallam, T.; Lee, K.; McEvoy, N.; Duesberg, G. S. Investigations of Vapour-Phase Deposited Transition Metal Dichalcogenide Films for Future Electronic Applications. *Solid. State. Electron.* **2016**, *125*, 39−51.

(21) Gatensby, R.; McEvoy, N.; Lee, K.; Hallam, T.; Berner, N. C.; Rezvani, E.; Winters, S.; O'Brien, M.; Duesberg, G. S. Controlled Synthesis of Transition Metal Dichalcogenide Thin Films for Electronic Applications. *Appl. Surf. Sci.* **2014**, *297*, 139−146.

(22) Lee, K.; Gatensby, R.; McEvoy, N.; Hallam, T.; Duesberg, G. S. High-Performance Sensors Based on Molybdenum Disulfide Thin Films. *Adv. Mater.* **2013**, *25*, 6699−6702.

(23) Lee, E.; Yoon, Y. S.; Kim, D. J. Two-Dimensional Transition Metal Dichalcogenides and Metal Oxide Hybrids for Gas Sensing. *ACS Sens.* **2018**, *3*, 2045−2060.

(24) Sajjad, M.; Montes, E.; Singh, N.; Schwingenschlögl, U. Superior Gas Sensing Properties of Monolayer PtSe 2. *Adv. Mater. Interfaces* **2017**, *4*, No. 1600911.

(25) Yim, C.; Lee, K.; McEvoy, N.; O'Brien, M.; Riazimehr, S.; Berner, N. C.; Cullen, C. P.; Kotakoski, J.; Meyer, J. C.; Lemme, M. C.; et al. High-Performance Hybrid Electronic Devices from Layered PtSe$_2$ Films Grown at Low Temperature. *ACS Nano* **2016**, *10*, 9550−9558.

(26) Nomani, M. W. K.; Shishir, R.; Qazi, M.; Diwan, D.; Shields, V. B.; Spencer, M. G.; Tompa, G. S.; Sbrockey, N. M.; Koley, G. Highly Sensitive and Selective Detection of NO2using Epitaxial Graphene on 6H-SiC. *Sens. Actuators, B* **2010**, *150*, 301−307.

(27) Yoon, H. J.; Jun, D. H.; Yang, J. H.; Zhou, Z.; Yang, S. S.; Cheng, M. M. C. Carbon Dioxide Gas Sensor Using a Graphene Sheet. *Sens. Actuators, B* **2011**, *157*, 310−313.

(28) Ricciardella, F.; Polichetti, T.; Vollebregt, S.; Alfano, B.; Massera, E.; Sarro, L. Analysis of a Calibration Method for Non-Stationary CVD Multi-Layered Graphene-Based Gas Sensors. *Nanotechnology* **2019**, *30*, No. 38.

(29) Ricciardella, F.; Massera, E.; Polichetti, T.; Miglietta, M. L.; Di Francia, G. A Calibrated Graphene-Based Chemi-Sensor for Sub Parts-per-Million NO$_2$ Detection Operating at Room Temperature. *Appl. Phys. Lett.* **2014**, *104*, No. 183502.

(30) Ricciardella, F.; Vollebregt, S.; Polichetti, T.; Alfano, B.; Massera, E.; Sarro, P. M. In *An Innovative Approach to Overcome Saturation and Recovery Issues of CVD Graphene-Based Gas Sensors*, Proceedings of IEEE Sensors, 2017.

(31) Ricciardella, F.; Vollebregt, S.; Polichetti, T.; Miscuglio, M.; Alfano, B.; Miglietta, M. L.; Massera, E.; Di Francia, G.; Sarro, P. M. Effects of Graphene Defects on Gas Sensing Properties towards NO2 Detection. *Nanoscale* **2017**, *9*, 6085−6093.

(32) Zhang, S.; Dong, N.; McEvoy, N.; OBrien, M.; Winters, S.; Berner, N. C.; Yim, C.; Li, Y.; Zhang, X.; Chen, Z.; et al. Direct Observation of Degenerate Two-Photon Absorption and Its Saturation in WS$_2$ and MoS$_2$ Monolayer and Few-Layer Films. *ACS Nano* **2015**, *9*, 7142−7150.

(33) O'Brien, M.; McEvoy, N.; Motta, C.; Zheng, J. Y.; Berner, N. C.; Kotakoski, J.; Elibol, K.; Pennycook, T. J.; Meyer, J. C.; Yim, C.; et al. Raman Characterization of Platinum Diselenide Thin Films. *2D Mater.* **2016**, *3*, No. 021004.

(34) Kim, W. Y.; Kim, H. J.; Hallam, T.; McEvoy, N.; Gatensby, R.; Nerl, H. C.; O'Neill, K.; Siris, R.; Kim, G. T.; Duesberg, G. S. Field-Dependent Electrical and Thermal Transport in Polycrystalline WSe$_2$. *Adv. Mater. Interfaces* **2018**, *5*, No. 1701161.

(35) Zhang, Y. I.; Zhang, L.; Zhou, C. Graphene and Related Applications. *Acc. Chem. Res.* **2013**, *46*, 2329−2339.

(36) Hallam, T.; Monaghan, S.; Gity, F.; Ansari, L.; Schmidt, M.; Downing, C.; Cullen, C. P.; Nicolosi, V.; Hurley, P. K.; Duesberg, G. S. Rhenium-Doped MoS$_2$ Films. *Appl. Phys. Lett.* **2017**, *111*, No. 203101.

(37) Donarelli, M.; Ottaviano, L. 2D Materials for Gas Sensing Applications: A Review on Graphene Oxide, MoS$_2$, WS$_2$ and Phosphorene. *Sensors* **2018**, *18*, 3638−3683.